

# NLO $Q^2$ -evolution of the nucleon's transversity distribution $h_1(x, Q^2)$ <sup>1</sup>

A. Hayashigaki, Y. Kanazawa and Yuji Koike  
*Graduate School of Science and Technology, Niigata University*  
*Ikarashi, Niigata 950-21, Japan*

## Abstract

We present a calculation of the two-loop anomalous dimension for the transversity distribution  $h_1(x, Q^2)$ ,  $\gamma_n^{h(1)}$ , in the MS scheme of the dimensional regularization. Because of the chiral-odd nature,  $h_1$  does not mix with the gluon distributions, and thus our result is the same for the flavor-singlet and nonsinglet distributions. At small  $n$  (moment of  $h_1$ ),  $\gamma_n^{h(1)}$  is significantly larger than  $\gamma_n^{f,g(1)}$  (the anomalous dimension for the nonsinglet  $f_1$  and  $g_1$ ), but approaches  $\gamma_n^{f,g(1)}$  very quickly at large  $n$ , keeping the relation  $\gamma_n^{h(1)} > \gamma_n^{f,g(1)}$ . This feature is in parallel to the relation between the one-loop anomalous dimension for  $f_1$  ( $g_1$ ) and  $h_1$ . We also show that this difference in the anomalous dimension between  $h_1$  and  $g_1$  leads to a drastic difference in the  $Q^2$ -evolution of those distributions in the small  $x$  region.

## 1 Introduction

The transversity distribution  $h_1(x, Q^2)$  is the third and the final twist-2 quark distribution function of the nucleon. It measures the probability in a transversely polarized nucleon to find a quark polarized parallel to the nucleon spin minus the probability to find it oppositely polarized. It thus supplies an information about the nucleon spin distribution not provided by the  $g_1$  distribution. Because of its chiral-odd nature,  $h_1$  can not be measured in the totally inclusive deep inelastic scattering (DIS), but it appears as a leading contribution in the transversely polarized nucleon-nucleon Drell-Yan process [1, 2, 3, 5], and the semi-inclusive DIS which detects pions [3],  $\Lambda$ 's [2, 4], and correlated two pions [6] in the final states.

Since  $h_1$  is twist-2, its  $Q^2$  evolution is described by the DGLAP equation [7]. The leading order (LO) splitting function for  $h_1$  has been known for some time [2]. In the recent literature, three papers [8, 9, 10] discussed the next-to-leading order (NLO)  $Q^2$  evolution of  $h_1$ : Vogelsang [8] carried out the light-cone gauge calculation of the two-loop splitting function [13] for  $h_1$  and converted it into the anomalous dimension. The present authors presented the Feynman gauge calculation of the two-loop anomalous dimension [9]. The final results of these two calculations in different formalisms agreed. These results were subsequently confirmed by [10] in the same formalism as [9]. These studies completed the whole list of the NLO anomalous dimension for the nucleon's all twist-2 distributions together with the known result for  $f_1$  [11, 12, 13] and  $g_1$  [14].

In this contribution, we discuss the NLO  $Q^2$ -evolution of  $h_1$  following our paper [9]. We

---

<sup>1</sup>In Proceedings of the Workshop "Deep Inelastic Scattering off Polarized Targets: Theory Meets Experiment", DESY-Zeuthen, Germany. Sep. 1-5, 1997. (Ed. J. Blümlein et al. DESY 97-200) pages 157-166. (presented by Y. Koike)

also present a numerical solution of the NLO evolution equation for  $h_1$ , comparing it with that of the  $g_1$  distribution. This latter part is a new result not presented in [9].

## 2 Twist-two operator for $h_1(x, Q^2)$ and its renormalization

The transversity distribution  $h_1(x, Q^2)$  of the nucleon is defined by the following relation [3]:

$$\int \frac{d\lambda}{2\pi} e^{i\lambda x} \langle PS | \bar{\psi}(0) \sigma_{\mu\nu} i\gamma_5 \psi(\lambda n) | Q | PS \rangle = 2 \left[ h_1(x, Q^2) (S_{\perp\mu} p_\nu - S_{\perp\nu} p_\mu) / M + h_L(x, Q^2) M (p_\mu n_\nu - p_\nu n_\mu) (S \cdot n) + h_3(x, Q^2) M (S_{\perp\mu} n_\nu - S_{\perp\nu} n_\mu) \right], \quad (2.1)$$

where  $|PS\rangle$  is the nucleon (mass  $M$ ) state specified by the four momentum  $P$  and the spin vector  $S$ , and two light-like vectors  $p$  and  $n$  are introduced by the relation,  $P^\mu = p^\mu + \frac{M^2}{2} n^\mu$  and  $pn = 1$ .  $S^\mu$  is decomposed as  $S^\mu = (S \cdot n) p^\mu + (S \cdot p) n^\mu + S_\perp^\mu$ . In (2.1), the gauge link operator to ensure the gauge invariance is suppressed.  $h_L$  and  $h_3$  are twist-3 and -4 distributions which are not in our interest here. The quark distributions  $h_{1,L,3}$  in (2.1) are defined for each quark flavor. The replacement of  $\psi \rightarrow C\bar{\psi}^T$  and  $\bar{\psi} \rightarrow -\psi^T C^{-1}$  defines anti-quark distributions  $\bar{h}_1(x, Q^2)$ , and it is related to  $h_1(x, Q^2)$  by the relation  $\bar{h}_1(x, Q^2) = -h_1(-x, Q^2)$ . Taylor expanding the both sides of (2.1) with respect to  $\lambda$ , one can relate the  $n$ -th moments of  $h_{1,L}$  to the following local operator:

$$\theta_{\mu\nu\mu_1\dots\mu_n} = \mathcal{S}_n \bar{\psi} i\gamma_5 \sigma_{\mu\nu} iD_{\mu_1} \dots iD_{\mu_n} \psi, \quad (2.2)$$

where  $\mathcal{S}_n$  denotes the symmetrization among  $\nu, \mu_1, \dots, \mu_n$ , and the covariant derivative  $D_\mu = \partial_\mu - igT^a A_\mu^a$  restores the gauge invariance. In particular, the  $n$ -th moment of  $h_1$  is related to a tower of the twist-2 operators:

$$\mathcal{M}_n[h_1(Q^2)] \equiv \int_{-1}^1 dx x^n h_1(x, Q^2) = \int_0^1 dx x^n \left[ h_1(x, Q^2) + (-1)^{n+1} \bar{h}_1(x, Q^2) \right], \quad (2.3)$$

$$\begin{aligned} \langle PS | \bar{\theta}_{\mu\nu\mu_1\dots\mu_n}(Q) \Delta^\nu \Delta^{\mu_1} \dots \Delta^{\mu_n} | PS \rangle \\ = \frac{2}{M} \mathcal{M}_n[h_1(Q^2)] \left( S_\mu \hat{P}^{n+1} - P_\mu \hat{S} \hat{P}^n + \frac{2}{n+2} M^2 \Delta_\mu \hat{S} \hat{P}^{n-1} \right), \end{aligned} \quad (2.4)$$

where  $\bar{\theta}_{\mu\nu\mu_1\dots\mu_n}$  is defined as the traceless part of  $\theta_{\mu\nu\mu_1\dots\mu_n}$  defined by the condition,

$$g^{\mu\mu_i} \bar{\theta}_{\mu\nu\mu_1\dots\mu_n} = g^{\nu\mu_i} \bar{\theta}_{\mu\nu\mu_1\dots\mu_n} = g^{\mu_i\mu_j} \bar{\theta}_{\mu\nu\mu_1\dots\mu_n} = 0, \quad (2.5)$$

and we introduced a null vector  $\Delta^\mu$  ( $\Delta^2 = 0$ ) which symmetrizes the indices  $\nu, \mu_1, \dots, \mu_n$  and kills off most of the trace terms in  $\bar{\theta}_{\mu\nu\mu_1\dots\mu_n}$  as usual.

For simplicity we symbolically use the notation  $O_n$  for  $\bar{\theta}_{\mu\nu\mu_1\dots\mu_n}$  in what follows in this section. The bare- ( $O_n^B$ ) and the renormalized- ( $O_n(\mu)$ ) composite operators are related by the renormalization constant  $Z_n(\mu)$  for  $O_n$  as

$$O_n(\mu) = Z_n^{-1}(\mu) O_n^B. \quad (2.6)$$

The scale dependence of  $O_n(\mu)$  is obtained by solving the renormalization group equation

$$\mu \frac{dO_n(\mu)}{d\mu} + \gamma_n(g(\mu))O_n(\mu) = 0, \quad (2.7)$$

where  $\gamma_n(g(\mu))$  is the anomalous dimension for the operator  $O_n(\mu)$  defined as

$$\gamma_n(g(\mu)) = \mu \frac{\partial}{\partial \mu} \ln Z_n(\mu). \quad (2.8)$$

This equation is solved to give

$$O_n(Q^2) = O_n(\mu^2) \exp \left[ - \int_{g(\mu^2)}^{g(Q^2)} dg \frac{\gamma_n(g)}{\beta(g)} \right]. \quad (2.9)$$

Up to next-to-leading order, the anomalous dimension  $\gamma_n(\mu)$  and the beta function  $\beta(g)$  can be expanded as

$$\gamma_n(g) = \frac{g^2}{16\pi^2} \gamma_n^{(0)} + \frac{g^4}{(16\pi^2)^2} \gamma_n^{(1)} + O(g^6), \quad (2.10)$$

$$\beta(g) = -\frac{g^3}{16\pi^2} \beta_0 - \frac{g^5}{(16\pi^2)^2} \beta_1 + O(g^7), \quad (2.11)$$

where the coefficients of the  $\beta$ -functions are well known;  $\beta_0 = 11 - (2/3)N_f$ ,  $\beta_1 = 102 - (38/3)N_f$ , with the number of quark flavor  $N_f$ . Inserting these equations into (2.9), one obtains the next-to-leading order evolution equation for the  $n$ -th moment of  $h_1$  as

$$\mathcal{M}_n[h_1(Q^2)] = R_n(Q^2, \mu^2) \mathcal{M}_n[h_1(\mu^2)], \quad (2.12)$$

$$R_n(Q^2, \mu^2) = \left( \frac{\alpha_s(Q^2)}{\alpha_s(\mu^2)} \right)^{\gamma_n^{(0)}/2\beta_0} \left[ 1 + \frac{\alpha_s(Q^2) - \alpha_s(\mu^2)}{4\pi} \frac{\beta_1}{\beta_0} \left( \frac{\gamma_n^{(1)}}{2\beta_1} - \frac{\gamma_n^{(0)}}{2\beta_0} \right) \right], \quad (2.13)$$

$$\frac{\alpha_s(Q^2)}{4\pi} = \frac{1}{\beta_0 \ln(Q^2/\Lambda^2)} \left[ 1 - \frac{\beta_1 \ln \ln(Q^2/\Lambda^2)}{\beta_0^2 \ln(Q^2/\Lambda^2)} \right]. \quad (2.14)$$

The LO evolution equation can be obtained by putting  $\beta_1$  and  $\gamma_n^{(1)}$  equal to zero in (2.13) and (2.14). This NLO effect in  $h_1$  has to be combined with the NLO effect in the hard cross section in the parton level to give a prediction for a relevant physical cross section in the NLO level.

### 3 Two-loop anomalous dimension for $h_1(x, Q^2)$

To obtain the renormalization constants for  $\bar{\theta}^{\mu\nu\mu_1 \dots \mu_n}$  in (2.4), we calculate the two-loop correction to the two-point function for  $\bar{\theta}$  in the Feynmann gauge with off-shell quark lines having the momentum  $p$  ( $p^2 < 0$ ). Those diagrams are shown in Fig. 1. Owing to the chiral-odd nature of  $h_1$ , it does not mix with the gluon distribution. Therefore Fermion loop diagrams peculiar to the flavor-singlet distribution do not contribute to the renormalization of  $h_1$ . The calculation of the two-loop Feynman diagrams is rather involved, and we refer the details of the calculation to our paper [9].

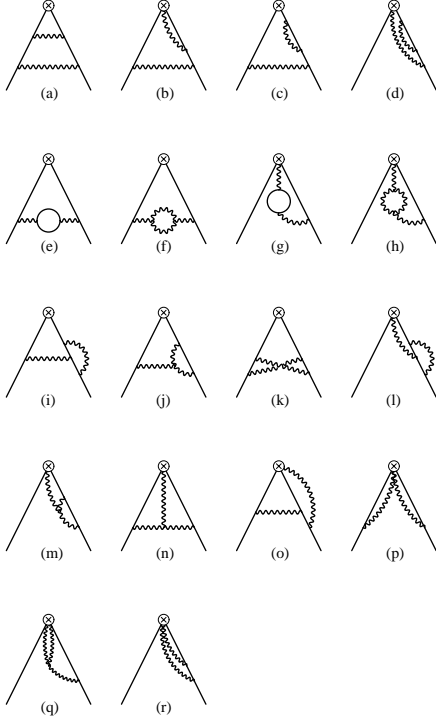


Fig. 1 : Two-loop corrections to the one-particle irreducible two-point Green function which imbeds the operator  $O_n^\mu \cdot \Delta$ .

In the  $\overline{\text{MS}}$  scheme, the final result for the two-loop anomalous dimension  $\gamma_n^{(1)}$  (2.10) for  $h_1$  reads

$$\begin{aligned}
\gamma_n^{h(1)} &= 4C_F^2 \left[ S_2(n+1) - 2S_1(n+1) - \frac{1}{4} \right] \\
&\quad + C_F C_G \left[ -16S_1(n+1)S_2(n+1) - \frac{58}{3}S_2(n+1) + \frac{572}{9}S_1(n+1) - \frac{20}{3} \right] \\
&\quad - 8 \left( C_F^2 - \frac{1}{2}C_F C_G \right) \left[ 4S_1(n+1) \left\{ S_2' \left( \frac{n+1}{2} \right) - S_2(n+1) - \frac{1}{4} \right\} - 8\tilde{S}(n+1) \right. \\
&\quad \left. + S_3' \left( \frac{n+1}{2} \right) - \frac{5}{2}S_2(n+1) + \frac{(1+(-1)^n)}{(n+1)(n+2)} + \frac{1}{4} \right] \\
&\quad + \frac{32}{9}C_F T_R \left[ 3S_2(n+1) - 5S_1(n+1) + \frac{3}{8} \right], \tag{3.1}
\end{aligned}$$

where

$$S_k(n) = \sum_{j=1}^n \frac{1}{j^k}, \tag{3.2}$$

$$S_k' \left( \frac{n}{2} \right) = \frac{1+(-1)^n}{2} S_k \left( \frac{n}{2} \right) + \frac{1-(-1)^n}{2} S_k \left( \frac{n-1}{2} \right), \tag{3.3}$$

$$\tilde{S}(n) = \sum_{j=1}^n \frac{(-1)^j}{j^2} S_1(j), \tag{3.4}$$

and  $C_F = \frac{N_c^2 - 1}{2N_c}$ ,  $C_G = N_c$ ,  $T_R = N_f/2$  with the number of color  $N_c$  and the number of quark-flavor  $N_f$ . Equation (3.1) shows  $\gamma_n^{h(1)} \sim \ln n$  at large  $n$  as was the case for  $\gamma_n^{f(1)}$  ( $\gamma_n^{(1)}$  for the nonsiglet  $f_1$  and  $g_1$ ) [12]. To compare their behavior, we plotted  $\gamma_n^{h,f(1)}$  for  $N_f = 3, 5$  in Fig. 2.

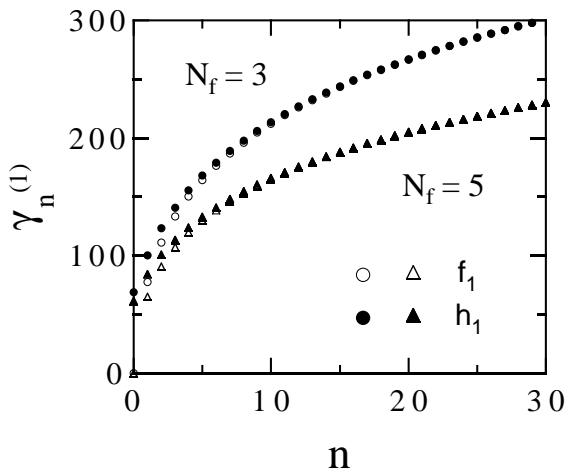


Fig. 2 : Two-loop anomalous dimension  $\gamma_n^{f,h(1)}$  for  $N_f = 3$  (circle) and  $N_f = 5$  (triangle).

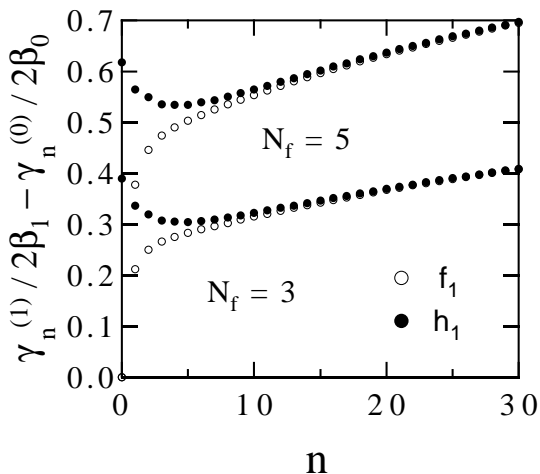


Fig. 3 :  $\gamma_n^{f,h(1)}/2\beta_1 - \gamma_n^{f,h(0)}/2\beta_0$  for  $N_f = 3, 5$ .

From Fig. 2, one sees clearly that at small  $n$   $\gamma_n^{h(1)}$  is significantly larger than  $\gamma_n^{f(1)}$  but approaches very quickly to  $\gamma_n^{f(1)}$ , keeping the condition  $\gamma_n^{h(1)} > \gamma_n^{f(1)}$ . This feature is the same as the one-loop anomalous dimensions  $\gamma_n^{h,f(0)}$  which reads

$$\gamma_n^{f(0)} = 2C_F \left( 1 - \frac{2}{(n+1)(n+2)} + 4 \sum_{j=2}^{n+1} \frac{1}{j} \right), \quad (3.5)$$

$$\gamma_n^{h(0)} = 2C_F \left( 1 + 4 \sum_{j=2}^{n+1} \frac{1}{j} \right), \quad (3.6)$$

and hence  $\gamma_n^{h(0)} > \gamma_n^{f(0)}$  for all  $n$ . Actually this tendency is even stronger for the two-loop case. We note that for  $n = 0$  the anomalous dimension for  $f_1$  is zero in all orders because of the Ward identity for the vector current. On the other hand,  $h_1$  projects onto the tensor operator  $\bar{\psi}\sigma^{\mu\nu}\psi$  for  $n = 0$ , for which there is no conservation law. Hence  $\gamma_0^{h(0,1)} \neq 0$ . From the difference between  $\gamma_n^{f(1)}$  and  $\gamma_n^{h(1)}$  at small  $n$ , we expect that the NLO effect leads to larger difference in the  $Q^2$ -evolution in the small- $x$  region. We note that the rightmost singularity of  $\gamma_n^{h(0)}$  is located at  $n = -2$  while that of  $\gamma_n^{h(1)}$  is at  $n = -1$ . Therefore, for the case of the transversity distribution, the NLO evolution renders the DGLAP asymptotics at  $x \rightarrow 0$  compatible with the Regge asymptotics [15].

Since the relevant quantities for the  $Q^2$ -evolution of the moments are  $\gamma_n^{(1)}/2\beta_1 - \gamma_n^{(0)}/2\beta_0$  (see (2.13)), we plotted it in Fig. 3 for  $N_f = 3$  and 5 cases. From this figure, one expects that at small  $n$  the NLO effect in the  $Q^2$  evolution is quite different between  $\mathcal{M}_n[h_1(Q^2)]$

and  $\mathcal{M}_n[f_1(Q^2)]$ . Since  $\gamma_n^{f(0,1)} \rightarrow 0$  as  $n \rightarrow 0$ ,  $\gamma_n^{f(1)}/2\beta_1 - \gamma_n^{f(0)}/2\beta_0$  abruptly drops to zero as  $n \rightarrow 0$ . But this is not the case for  $h_1$ : It shows a characteristic behavior as shown in Fig. 3.

As an example of the  $Q^2$ -evolution, we show in Fig. 4 (a) and (b) the  $Q^2$ -evolution of the tensor charge and the first moments, respectively, with the parameters  $N_f = 3$  and  $\Lambda = 0.232$  GeV in (2.14). (Here we are interested in the NLO effect in the anomalous dimension and the  $\beta$ -function, and thus we adopted the same value for the  $\Lambda$ -parameter in the LO and NLO evolution.)

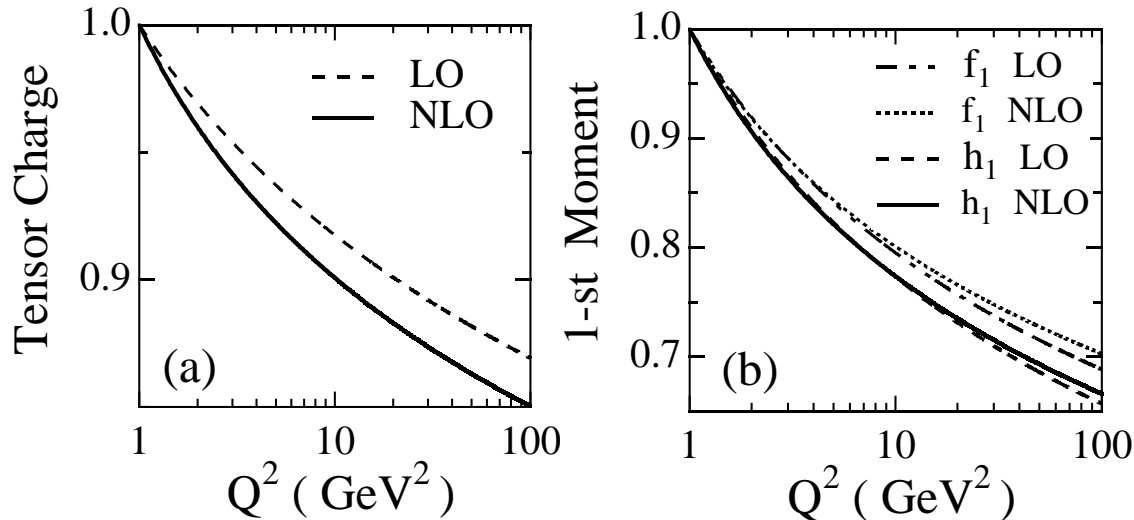


Fig. 4: (a) The LO and NLO  $Q^2$ -evolution of the tensor charge normalized at  $Q^2 = 1$  GeV<sup>2</sup>. (b) The LO and NLO  $Q^2$ -evolution of the first moment of  $h_1(x, Q^2)$  and  $f_1(x, Q^2)$  normalized at  $Q^2 = 1$  GeV<sup>2</sup>.

They are normalized at  $Q^2 = 1$  GeV<sup>2</sup>. At  $n = 0$ , only diagrams (e), (f), (i), (j), (k) in Fig. 1 survive. They give the anomalous dimension for the tensor charge as

$$\begin{aligned} \gamma_0^{h(1)} &= -19C_F^2 + \frac{257}{9}C_FC_G - \frac{52}{9}C_FT_R \\ &= \frac{724}{9} - \frac{104}{27}N_f. \end{aligned} \quad (3.7)$$

From Fig. 4(a), we can compare the LO and the NLO  $Q^2$ -evolution of the tensor charge of the nucleon. One sees that the NLO effect is sizable as is expected from Fig. 3. In Fig. 4(b), we plotted the LO and NLO  $Q^2$ -evolution both for  $\mathcal{M}_1[f_1(Q^2)]$  (nonsinglet) and  $\mathcal{M}_1[h_1(Q^2)]$ . Although the NLO effect in the anomalous dimension (the second factor in the right hand side of (2.13)) makes this ratio smaller, the NLO effect in the coupling constant (the first factor in the right hand side of (2.13)) completely cancels this effect. For  $f_1$ , the latter effect is actually larger than the former effect. As is shown in these examples, the NLO effect on each moment is not large. We will see, however, that it is significant for the distribution function itself in the next section.

## 4 $Q^2$ -evolution of $h_1$

To see a generic feature of the actual NLO  $Q^2$  evolution of  $h_1$ , we have applied the result of the two-loop anomalous dimension to a reference distribution function of  $h_1$ . In the nonrelativistic kinematics,  $h_1 = g_1$ , although the motion of quarks in the nucleon is not expected to be nonrelativistic. A bag model calculation suggests  $h_1$  is not very different from  $g_1$  at a low energy hadronic scale. We therefore assume that  $h_1(x, Q^2)$  is identical to a  $g_1(x, Q^2)$  distribution of Glück, Reya, Stratmann and Vogelsang (GRSV) [16] (standard scenario) at a low energy scale.

We first recall the general formalism of the NLO  $Q^2$ -evolution. Corresponding to the splitting of a quark into an anti-quark, there are terms proportional to  $(-1)^{n+1}$  such as those caused from  $S'_k$  and  $\tilde{S}$  in the anomalous dimension (3.1). One can thus write for  $R_n(Q^2, \mu^2)$  in (2.13) as

$$R_n(Q^2, \mu^2) = R_n^{qq}(Q^2, \mu^2) + (-1)^{n+1} R_n^{q\bar{q}}(Q^2, \mu^2). \quad (4.1)$$

We solve the evolution equation (2.12) with (2.3) and (4.1) for  $n = \text{even}$  and odd cases by analytically continuing them to all  $n$ . This gives the  $Q^2$ -evolution for the two combinations  $h_1(x, Q^2) \pm \bar{h}_1(x, Q^2)$ . Numerical solution was obtained following the method of [12]. We have checked that the method works sufficiently accurately in the  $x > 0.05$  region for the NLO evolution.

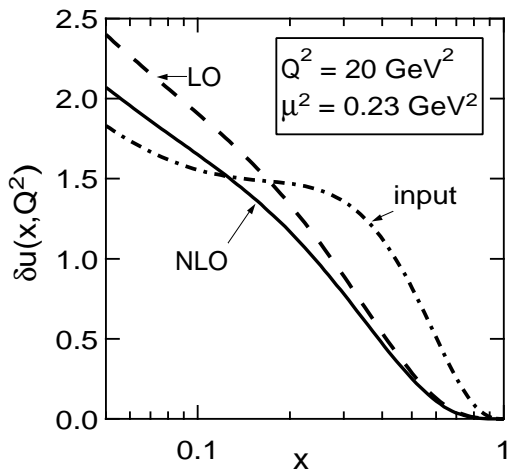


Fig. 5: The LO and NLO  $Q^2$ -evolution for the  $u$ -quark transversity distribution  $\delta u$ , starting from the same input function.

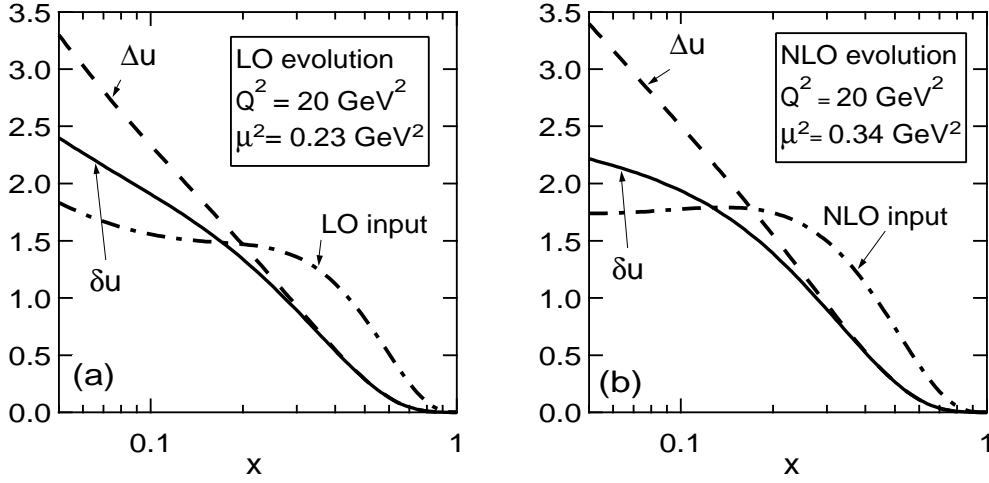


Fig. 6: (a) Comparison of the LO  $Q^2$ -evolution of  $\delta u(x, Q^2)$  and  $\Delta u(x, Q^2)$ . (b) Comparison of the NLO  $Q^2$ -evolution of  $\delta u(x, Q^2)$  and  $\Delta u(x, Q^2)$ .

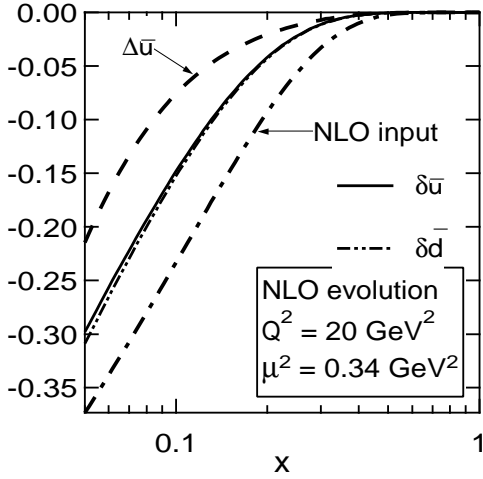


Fig. 7. Comparison of the NLO  $Q^2$ -evolution of  $\delta \bar{u}(x, Q^2)$ ,  $\delta \bar{d}(x, Q^2)$  and  $\Delta \bar{u}(x, Q^2)$ .

To see the magnitude of the NLO effect, we first applied the LO and NLO evolution of  $h_1$  to the same input function. As an input function we have chosen here the GRSV LO  $g_1$  distribution function at  $\mu^2 = 0.23 \text{ GeV}^2$ , which is the starting distribution of [16]. Figure 5 shows the result for the  $u$ -quark transversity distribution  $\delta u(x, Q^2)$  evolved to  $Q^2 = 20 \text{ GeV}^2$ . The NLO effect is significant especially in the small- $x$  region. The same tendency was observed for the other transversity distributions.

To compare the  $Q^2$ -evolution of the transversity distribution and the  $g_1$ -distribution, we show in Fig. 6 (a) and (b), respectively, the LO and NLO  $Q^2$ -evolution of  $\delta u$  and  $\Delta u$  ( $g_1$  for  $u$ -quark), starting from the GRSV LO and NLO input function for  $\Delta u$  given at  $Q^2 = 0.23$  and  $0.34 \text{ GeV}^2$ . Although the LO evolution leads to a significant difference between  $\delta u$



and  $\Delta u$  at  $Q^2 = 20 \text{ GeV}^2$ ,<sup>2</sup> this feature is even more conspicuous in the NLO evolution, in particular, in the small- $x$  region. This is expected from the behavior of the anomalous dimension. (Although the evolution of  $\Delta u$  shown in Fig. 6 is receiving some effect from the mixing with the gluon distribution, flavor-nonsinglet and valence distributions also show the same tendency.)

In Fig. 7, we compare the NLO  $Q^2$ -evolution of  $\delta\bar{u}$ ,  $\delta\bar{d}$  and  $\Delta\bar{u}$ , starting from the same input distribution function (GRSV NLO input function for the sea quark distribution for  $g_1$ ). The difference between  $\delta\bar{u}$  and  $\Delta\bar{u}$  is again significant. Although the input sea quark distribution is assumed to be flavor symmetric ( $\delta\bar{u} = \delta\bar{d}$  at  $Q^2 = 0.34 \text{ GeV}^2$ ), the NLO evolution leads to a violation of this symmetry because of the presence of  $R_n^{q\bar{q}}(Q^2, \mu^2)$  in (2.13). However, this effect is very small as can be seen from Fig. 7.<sup>3</sup>

## 5 Summary and outlook

In this work, we have carried out a Feynmann gauge calculation of the two-loop anomalous dimension for the transversity distribution  $h_1(x, Q^2)$  in the  $\overline{\text{MS}}$  scheme of the dimensional regularization. This completes the calculation of the anomalous dimensions for all the twist-2 distributions of the nucleon in the NLO level. We found  $\gamma_n^{h(1)}$  is significantly larger than the  $\gamma_n^{f,g(1)}$  (nonsinglet anomalous dimension for  $f_1$  and  $g_1$ ) at small  $n$ , but approaches very quickly to  $\gamma_n^{f,g(1)}$  at large  $n$ , keeping the condition  $\gamma_n^{h(1)} > \gamma_n^{f,g(1)}$ . The NLO effect in the anomalous dimension leads to a drastic difference in the  $Q^2$ -evolution between  $h_1$  and  $g_1$ . The NLO parton distribution function has to be combined with the NLO short distance cross section in the same factorization scheme to give a prediction for a physical quantity. For the transversely polarized Drell-Yan process, the latter has been calculated in [8, 19]. Combining these results, the NLO calculation of the double spin asymmetry for the Drell-Yan process has been presented in a recent work [18]. We hope the peculiar feature of the  $h_1$  distribution discussed in these works will be measured in the future collider experiments.

### Acknowledgement

This work is supported in part by RIKEN. We thank M. Stratmann and W. Vogelsang for providing us with the Fortran code of their  $g_1$  distribution.

## References

- [1] J.P. Ralston and D.E. Soper, Nucl. Phys. **B152**, 109 (1979).
- [2] X. Artru and M. Mekhfi, Z. Phys. **C45** 669 (1990); Nucl. Phys. **A532** (1991) 351c.
- [3] R.L. Jaffe and X. Ji, Phys. Rev. Lett. **67**, 552 (1991); Phys. Rev. Lett **71**, 2547 (1993).
- [4] R.L. Jaffe, Phys. Rev. **D54**, 6581 (1996).
- [5] J.L. Cortes, B. Pire and J.P. Ralston, Z. Phys. **C55**, 409 (1992).

---

<sup>2</sup>This difference was also pointed out in [17].

<sup>3</sup>This point is also discussed in [18]. At the time of the workshop, we reported this effect is sizable for  $h_1$  compared with  $g_1$  case. However, our numerical solution at that time turned out to be unreliable in the small  $x$  region ( $x < 0.05$ ).

- [6] R.L. Jaffe, X. Jin and J. Tang, hep-ph/9709322.
- [7] V.N. Gribov and L.N. Lipatov, Sov. J. Nucl. Phys. **15**, 438 (1972), G. A. Altarelli and G. Parisi, Nucl. Phys. **B126**, 298 (1977), Yu. L. Dokshitzer, Sov. Phys. JETP **46**, 641 (1977).
- [8] W. Vogelsang, hep-ph/9706511, June 25.
- [9] A. Hayashigaki, Y. Kanazawa, Y. Koike, hep-ph/9707208, July 1. Phys. Rev. **D** in press. Submitted on June 23.
- [10] S. Kumano and M. Miyama, hep-ph/9706420, Phys. Rev. **D56**, R2504 (1997), received on June 19. The first version of this paper was posted to hep-ph on June 19. However, it was wrong and presented the result in a very complicated nonfinal form. Later after [9] appeared on hep-ph, the authors of this reference corrected the result and replaced their preprint on hep-ph on July 26. This revised version was eventually published in Phys. Rev. **D** with no revised date explicitly shown. We regret the authors of this reference did not clarify this point in their note added in the proof. For example, in their first version of the paper, the final results in eqs.(A4)-(A8) and (A9) itself did not exist, and furthermore their long intermediate results in (A4)-(A6) were clearly different from the revised ones.
- [11] E.G. Floratos, D.A. Ross and C.T. Sachrajda, Nucl. Phys. **B129**, 66 (1977); **B139**, 545 (1978) (E); Nucl. Phys. **B152**, 493 (1979).
- [12] A. Gonzalez-Arroyo, C. Lopez and F.J. Yndurain, Nucl. Phys. **B153**, 161 (1979).
- [13] G. Curci, W. Furmanski and R. Petronzio, Nucl. Phys. **B175**, 27 (1980), W. Furmanski and R. Petronzio, Phys. Lett **97B**, 437 (1980).
- [14] R. Mertig, W.L. van Neerven, Z. Phys. **C70** 637 (1996); W. Vogelsang, Phys. Rev. **D54** 2023 (1996); Nucl. Phys. **B475**, 47 (1996).
- [15] R. Kirschner, L. Mankiewicz, A. Schäfer and L. Szymanowski, Z. Phys. **C74**, 501 (1997); R. Kirschner, proceedings of this workshop, hep-ph/9710253.
- [16] M. Glück, E. Reya, M. Stratmann and W. Vogelsang, Phys. Rev. **D53**, 4775 (1996).
- [17] V. Barone, T. Calarco and A. Drago, Phys. Rev. **D56**, 527 (1997).
- [18] O. Martin, A. Schäfer, M. Stratmann, and W. Vogelsang, hep-ph/9710300.
- [19] A.P. Contogouris, B. Kamal and Z. Merebashvili, Phys. Lett. **B337**, 169 (1994); B. Kamal, Phys. Rev. **D53**, 1142 (1996).